

Reprinted from

JOURNAL OF HYDROLOGY

Journal of Hydrology 188-189 (1997) 516-535

The role of the Sahelian biosphere on the water and the CO₂ cycle during the HAPEX-Sahel Experiment

B.A. Monteny^{a,*}, J.P. Lhomme^a, A. Chehbouni^a, D. Trouffleau^b, M. Amadou^c,
M. Sicot^a, A. Verhoef^d, S. Galle^a, F. Said^e, C.R. Lloyd^f

^aORSTOM—Hydrology, BP 5045, 34032 Montpellier, France

^bCEMAGREF, Maison de la Télédetection, 34093 Montpellier Cedex 5, France

^cINRAN—BP 429, Niamey, Niger

^dAgricultural University Wageningen, Department of Meteorology, Wageningen, The Netherlands

^eUniversité de Toulouse, Laboratoire d'Aerologie, Toulouse, France

^fInstitute of Hydrology, Wallingford OX10 8BB, UK

Fonds Documentaire IRD



010021616



ELSEVIER

Fonds Documentaire IRD

Cote: B* 21616 Ex: 7

Editors

R. Krzysztofowicz, Charlottesville, VA, USA
G. Teutsch, Tübingen, Germany
G. Vachaud, Grenoble, France
P. van Cappellen, Atlanta, GA, USA

Associate Editors

J.A. Barker, London, UK
A. Becker, Berlin, Germany
R. Berndtsson, Lund, Sweden
B. Bobee, Quebec, Que., Canada
I.R. Calder, Wallingford, UK
R.T. Clarke, Porto Alegre, Brazil
M. Franchini, Bologna, Italy
M. French, Louisville, KY, USA
E.O. Frind, Waterloo, Ont., Canada
J.H.C. Gash, Wallingford, UK
K.P. Georgakakos, San Diego, CA, USA
S. Guo, Wuhan, People's Republic of China
Tissa H. Illangasekare, Boulder, CO, USA
M.L. Kavvas, Davis, CA, USA
W.E. Kelly, Washington, DC, USA
W.F. Krajewski, Iowa City, IA, USA
L.S. Kuchment, Moscow, Russia
D.R. Maidment, Austin, TX, USA
A.I. Mc Kerchar, Christchurch, New Zealand
U. Moiseo, Pavia, Italy
E.M. Murphy, Richland, WA, USA
C. Neal, Wallingford, UK
A.J. Peck, Subiaco, W.A., Australia
H.N. Phien, Bangkok, Thailand
H. Savenije, Delft, Netherlands
G.A. Schultz, Bochum, Germany
H.M. Seip, Oslo, Norway
W.J. Shuttleworth, Tucson, AZ, USA
M. Sivapalan, Nedlands, W.A., Australia
M. Sophocleous, Lawrence, KS, USA
C.I. Steefel, Tampa, FL, USA
D. Stephenson, Johannesburg, South Africa
Y. Tagutschi, Tsukuba, Japan
A. van der Beken, Brussels, Belgium

Scope of the journal

The *Journal of Hydrology* publishes original research papers and comprehensive reviews in all the subfields of the hydrological sciences. These comprise, but are not limited to the physical, chemical, biogeochemical, stochastic and systems aspects of surface and groundwater hydrology, hydrometeorology and hydrogeology. Relevant topics in related disciplines such as climatology, water resource systems, hydraulics, agrohydrology, geomorphology, soil science, instrumentation and remote sensing, civil and environmental engineering are also included. Papers have empirical, theoretical and applied orientations.

Publication information

Journal of Hydrology (ISSN 0022-1694). For 1997 volumes 187-199 are scheduled for publication. Subscription prices are available upon request from the publishers. Subscriptions are accepted on a prepaid basis only and are entered on a calendar year basis. Issues are sent by surface mail except to the following countries where air delivery via SAL (Surface Air Lifted) mail is ensured: Argentina, Australia, Brazil, Canada, Hong Kong, India, Israel, Japan*, Malaysia, Mexico, New Zealand, Pakistan, China, Singapore, South Africa, South Korea, Taiwan, Thailand, USA. For all other countries airmail rates are available upon request. Claims for missing issues must be made within 6 months of our publication (mailing) date.

For orders, claims, product enquiries (no manuscript enquiries) please contact the Customer Support Department at the Regional Sales Office nearest to you: **New York**, Elsevier Science, P.O. Box 945, New York, NY 10159-0945, USA. Tel: (+1) 212-633-3730, [Toll Free number for North American customers: 1-888-4ES-INFO (437-4636)], Fax: (+1) 212-633-3680, E-mail: usinfo-f@elsevier.com - **Amsterdam**, Elsevier Science, P.O. Box 211, 1000 AE Amsterdam, The Netherlands. Tel: (+31) 20-485-3757, Fax: (+31) 20-485-3432, E-mail: nlinfo-f@elsevier.nl - **Tokyo**, Elsevier Science, 9-15, Higashi-Azabu, Minato-ku, Tokyo 106, Japan. Tel: (+81) 3-5561-5033, Fax: (+81) 3-5561-5047, E-mail: kyf04035@niftyserve.or.jp - **Singapore**, Elsevier Science, No. 1 Temasek Avenue, #17-01 Millenia Tower, Singapore 039192. Tel: (+65) 434-3727, Fax: (+65) 337-2230, E-mail: asiainfo@elsevier.com.sg

Advertising Information

Advertising orders and enquiries may be sent to: **International**: Elsevier Science, Advertising Department, The Boulevard, Langford Lane, Kidlington, Oxford OX5 1GB, UK; Tel: (0) 1865 843565; Fax: (0) 1865 843952. **USA and Canada**: Weston Media Associates, Dan Lipner, P.O. Box 1110, Greens Farms, CT 06436-1110, USA; Tel: (203) 261 2500; Fax: (203) 261 0101. **Japan**: Elsevier Science Japan, Advertising Department, 1-9-15 Higashi-Azabu 1-chome, Minato-ku, Tokyo 106, Japan; Tel: (3) 5561 5033; Fax: (3) 5561 5047.

Copyright © 1997 Elsevier Science B.V. All rights reserved.

0022-1694/97/\$17.00

This journal and the individual contributions contained in it are protected by the copyright of Elsevier Science B.V., and the following terms and conditions apply to their use:

Photocopying

Single photocopies of single articles may be made for personal use as allowed by national copyright laws. Permission of the publisher and payment of a fee is required for all other photocopying, including multiple or systematic copying, copying for advertising or promotional purposes, resale, and all forms of document delivery. Special rates are available for educational institutions that wish to make photocopies for non-profit educational classroom use.

In the USA, users may clear permissions and make payment through the Copyright Clearance Center, Inc., 222 Rosewood Drive, Danvers, MA 01923, USA. In the UK, users may clear permissions and make payment through the Copyright Licensing Agency Rapid Clearance Service (CLARCS), 90 Tottenham Court Road, London W1P 0LP, UK. In other countries where a local copyright clearance centre exists, please contact it for information on required permissions and payments.

Derivative Works

Subscribers may reproduce tables of contents or prepare lists of articles including abstracts for internal circulation within their institutions. Permission of the publisher is required for resale or distribution outside the institution.

Permission of the publisher is required for all other derivative works, including compilations and translations.

Electronic Storage

Permission of the publisher is required to store electronically any material contained in this journal, including any article or part of an article. Contact the publisher at the address indicated.

Except as outlined above, no part of this publication may be reproduced, stored in a retrieval system or transmitted in any form or by any means, electronic, mechanical, photocopying, recording or otherwise, without prior written permission of the publisher.

Disclaimers

No responsibility is assumed by the publisher for any injury and/or damage to persons or property as a matter of products liability, negligence or otherwise, or from any use or operation of any methods, products, instructions or ideas contained in the material herein.

Although all advertising material is expected to conform to ethical (medical) standards, inclusion in this publication does not constitute a guarantee or endorsement of the quality or value of such product or of the claims made of it by its manufacturer.

© The paper used in this publication meets the requirements of ANSI/NISO Z39.48-1992 (Permanence of Paper).

Printed in The Netherlands



ELSEVIER

Journal of Hydrology 188–189 (1997) 516–535

Journal
of
Hydrology

The role of the Sahelian biosphere on the water and the CO₂ cycle during the HAPEX-Sahel Experiment

B.A. Monteny^{a,*}, J.P. Lhomme^a, A. Chehbouni^a, D. Troufseau^b, M. Amadou^c,
M. Sicot^a, A. Verhoef^d, S. Galle^a, F. Saïd^e, C.R. Lloyd^f

^aORSTOM—Hydrology, BP 5045, 34032 Montpellier, France

^bCEMAGREF, Maison de la Télédétection, 34093 Montpellier Cedex 5, France

^cINRAN—BP 429, Niamey, Niger

^dAgricultural University Wageningen, Department of Meteorology, Wageningen, The Netherlands

^eUniversité de Toulouse, Laboratoire d'Aerologie, Toulouse, France

^fInstitute of Hydrology, Wallingford OX10 8BB, UK

Abstract

The HAPEX-Sahel experiment was organized to investigate the impact of water, energy and CO₂ fluxes at the soil–vegetation–atmosphere interface on climate processes in the Sahelian region. Measurements of the energy balance components, CO₂ flux and soil moisture were conducted over a savanna area at the East Central Supersite of the one degree square during a 3 month period in 1992. The aim of this particular investigation was to understand the role of surface conditions (i.e. vegetation and moisture) in the partitioning of available energy at the surface into sensible and latent heat flux. It also aimed to improve the understanding of how water and carbon cycles are affected by vegetation functioning, soil water availability and atmospheric demand. The analysis presented in this paper showed that the relative contribution of the soil and the vegetation to latent heat flux varies intimately with the temporal rainfall distribution and the growth of the savanna grass species, which is more sensitive to the distribution of precipitation than to its amount. Finally, semi-empirical parameterizations were developed to formulate (1) the daily evapotranspiration rate of the savanna in terms of available energy at the surface and soil water content, and (2) the instantaneous carbon uptake in terms of photosynthetically active radiation received at the surface and soil water availability.

* Corresponding author.



1. Introduction

It has been increasingly apparent in recent years that accurate predictions of possible climate change and its consequences in semi-arid regions rely on understanding the exchange mechanisms of water, energy and CO₂ at the land surface–atmosphere interface. The key issue is to parameterize correctly these processes in mesoscale models. This requires an accurate understanding of the linkage between the forcing factors (climatic as well as human) and the relevant land-surface processes at different time–space scales.

Recently, several multidisciplinary field experiments have been conducted over different biome types. In this context, the HAPEX-Sahel experiment was organized during summer 1992 in the southwest of Niger. The aim of the experiment is to improve the parameterization of the land surface processes in general circulation models (GCMs) by combining remote sensing techniques and hydrological modelling (Goutorbe et al., 1994; Lhomme et al., 1994a, Lhomme et al., 1994b; Prince et al., 1995). A preliminary investigation took place in the same area within the framework of the Sahelian Energy Budget EXperiment (SEBEX), where emphasis was mostly on the water cycle (Gash et al., 1991; Wallace et al., 1991) without coupling it to the carbon cycle.

In this study, the temporal variability of surface fluxes in response to climatic forcing and surface conditions was investigated, especially the flux of water and of CO₂ of the savanna area in the Central East Site of the HAPEX one degree square. Data were collected with a Bowen ratio based system to study the dynamic interactions between the Sahelian savanna and the atmosphere. Some semi-empirical parameterizations were developed to compute the exchange rates between the savanna area and the atmosphere using conventional meteorological data. Their evolutions give a comprehensive insight into the water and CO₂ cycles; they also affect the surface boundary-layer characteristics at regional scale as a source or a sink.

2. Material and methods

2.1. Climatic conditions

The East Central Supersite is located 65 km east of Niamey, near Banizoumbou village (13°31'931N, 2°39'636E). Climate variables were monitored routinely at a long-term meteorological station at Banizoumbou. The development of the climatic conditions is related largely to the shift of the Intertropical Convergence Zone (ITCZ) over the Sahelian region (Leroux, 1983; Monteny, 1993; Goutorbe et al., 1994). Fig. 1 presents the development of the climatic conditions during 1992. From May until the beginning of October (Decade 13–29), most of the Sahelian region was under the influence of moist southwesterly air masses. Dew-point temperature increased from 5°C to 22°C and nearly equalled the minimum temperature; therefore dew could have occurred on the leaves of plants in the morning hours. The rainy season began in mid-July and ended in mid-September. The maximum rainfall occurred in August and cloud cover affected the incident solar radiation. During 1992, the rainy season was particularly short, with a total amount of 424 mm at Banizoumbou.

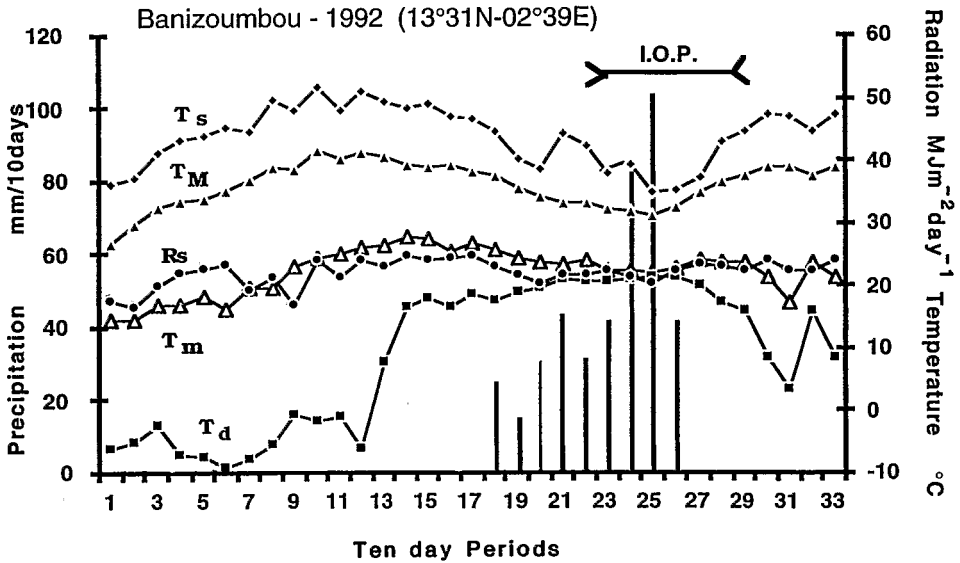


Fig. 1. Climate conditions during 1992 at Banizoumbou ($13^{\circ}31'931N$, $2^{\circ}39'636E$), 65 km east of Niamey, Niger. The East Central site received about two-thirds of the average annual rainfall in 1992. T_d , Dew-point temperature; T_m , minimum temperature; T_M , maximum temperature; T_s , maximum soil temperature (2 cm); R_s , total incoming solar radiation; vertical bar, precipitation.

2.2. Site description

The region is covered mainly by aeolian sand of variable depth depending on the underground laterite plateau (see Goutorbe et al. (1997) and the site report (Monteny, 1993)). The savanna area consists of scattered bushes covering 17% of the area, underlain by a sparse grass layer of different species seeding at different periods during the rainy season. For the same total amount of precipitation, biomass production can be completely different from one year to another owing to the differential dynamics of the plant species induced by the rainfall event distribution during the wet season. The rates of seeding and growth (leaf area and density), and the timing of phenological development of the species are dependent on the soil water content.

The grass layer of the savanna ecosystem is composed essentially of annual plants with a number of C_3 species growing in competition with C_4 species. Several species (*Aristida mutabilis*, (C4); *Aristida adscensionis*, (C4); *Cenchrus biflorus*, (C4); *Mitarcarpus scaber*, (C3); *Tribulus terrestris* (C3)) are in competition after seed germination following the first heavy rainfall (Adamou, 1992; E. Delabre, personal communication, 1994). With more regular precipitation events, other plant species appear: *Zornia glochidiata*, (C3); *Ctenium elegans*, (C4); *Digitaria gayana*, (C4); *Eragrostis tremula*, (C4); *Dactyloctenium aegyptium*, (C4); *Indigofera aspera* (C3); *Mitarcarpus scaber* (C3). The importance of variable growth rates among species has to be considered as a primary forcing characteristic for establishing the composition and structure of vegetation. Here, the grass presents generally erect leaves.

With the start of the dry season in mid September, young plants dry out without bearing fruit and for the other established plants, senescence may appear 1–3 weeks after the last rainfall event. Table 1 gives information about the evolution of the grass layer characteristics (height, leaf area index (LAI) and biomass) as well as the evolution of the soil water content.

2.3. Measurements of the energy budget components

Micrometeorological methods are well suited for measuring the vertical evapotranspiration flux and the carbon assimilation rate over land surfaces without altering the surface environmental conditions. Bowen ratio–energy balance (BREB) and eddy correlation techniques were used to measure the evapotranspiration flux and the CO₂ flux over vegetated surfaces.

2.3.1. Components of the energy budget

2.3.1.1. *Energy budget.* The energy budget of a vegetated surface, when small storage terms are ignored, can be written for steady-state conditions as

$$R_n - G = \lambda E + H + \mu A \quad (1)$$

where R_n is the net radiation flux density and G is the soil heat flux density. The available energy at the surface, $R_n - G$, provides the energy for the latent heat flux density, λE and sensible heat flux density, H (with E the evapotranspiration and λ the latent heat of vaporization). μA is the carbon assimilation rate (photochemical energy fixed by photosynthesis), where A is the net assimilation rate ($\text{mol m}^{-2} \text{s}^{-1}$) and μ is the heat of formation of carbohydrate per unit amount of CO₂ assimilated A ($\text{J mol}^{-1} \text{CO}_2$). This last term is generally neglected when carbon fluxes are not measured.

Another way of evaluating the effect of soil moisture availability on evapotranspiration rate is to consider the Priestley–Taylor coefficient α as a function of the soil water content. The Priestley–Taylor equation, which estimates the regional evaporation, based upon the available energy, is written (Priestley and Taylor, 1972)

$$\lambda E = \alpha \lambda E_0 = \alpha \left(\frac{s}{s + \gamma} \right) (R_n - G) \quad (2)$$

Table 1
Surface characteristics of the savanna grass layer for selected days

Day of year	Height (m)	LAI (total)	LAI (green)	Biomass (kg ha ⁻¹)	Soil water content (mm 0.60 m ⁻¹ depth)
258	0.38	0.47	0.47	727	39
260					51 max.
266	0.49	0.7	0.7	1062	36
272	0.55	0.95	0.8	1262	21
286	0.65	0.9	0.4	1374	13

where α is unitless coefficient close to 1.25 for well-watered vegetation, λE_0 is the equilibrium evaporation depending on available energy, s is the slope of the curve relating saturation vapour pressure of air to temperature and γ is the psychrometric constant.

The coefficient α , calculated as the ratio E/E_0 of measured evapotranspiration to equilibrium evapotranspiration, can be used to evaluate the evapotranspiration rate of a semi-arid region (Stannards, 1993). The value of α is related to the canopy surface resistance r_s through the soil water content S/S_m . When the soil water availability decreases and the vegetation is stressed, α decreases. An empirical expression can be used to relate α to the relative soil water content (De Bruin, 1983; Monteny and Casenave, 1989; Nichols and Cuenca, 1993)

2.3.1.2. *Radiation budget.* The radiation budget of the savanna vegetation is

$$R_n = R_s - R_r + R_a - \epsilon \sigma T_s^4 \quad (3)$$

where R_s the incoming shortwave radiation, R_r the reflected shortwave solar radiation, R_a the incoming long wave radiation and $\epsilon \sigma T_s^4$ the emitted longwave radiation, with σ the Stefan–Boltzmann constant, ϵ the emissivity (assumed to be equal to unity), and T_s the surface temperature (K). R_s and the photosynthetically active radiation (PAR) R_p (400–720 nm) of the incoming solar radiation were measured with a Kipp CM6 pyranometer (Kipp and Zonen, Delft, Netherlands), calibrated against an Eppley radiometer (Eppley Lab. Inc., RI, USA), and a quantum flux density sensor (Campbell Scientific, Shephed, UK), respectively. These radiation data were recorded continuously at the meteorological station near Banizoumbou.

2.3.2. *Experimental fields and flux stations (Bowen ratio apparatus)*

2.3.2.1. *Flux measurements: Bowen ratio β coupled with the energy budget.* For many years, the Bowen ratio technique has been used in conjunction with the energy balance to assess areal evaporation and CO_2 downward flux (Denmead et al., 1971; Jarvis et al., 1976; Denmead and Bradley, 1985; Baldocchi et al., 1988; Verma et al., 1989; Cellier and Olioso, 1993; Stannards et al., 1994).

Under conditions of steady state, horizontal homogeneity and equality of the aerodynamic turbulent resistances of sensible and latent heat flux and CO_2 assimilation near the surface, the Bowen ratio, $\beta = H/\lambda E$, can be derived from measurements of the vertical gradient of air temperature, dT , and of the water vapour pressure, de , in the atmosphere:

$$\beta = \frac{dT}{de}$$

The available energy $R_n - G$ can be measured directly, and sensible heat and latent heat fluxes can be obtained from the energy budget (Eq. (1)) (Denmead and Bradley, 1985; Anderson and Verma, 1986; Cellier and Olioso, 1993):

$$\lambda E = \frac{R_n - G}{1 + \beta} \quad (4)$$

$$H = \beta \frac{(R_n - G)}{1 + \beta} \quad (5)$$

The evaporative fraction, $\lambda E/(R_n - G)$, characterizes the energy partitioning over land surfaces.

In the savanna area, 4 km from Banizoumbou, two flux stations were installed: one station in the savanna area covered by short annual grass with scattered woody perennial shrubs of *Guiera senegalensis* (the dominant savanna vegetation), the other station in a large area of sparse grass without bushes. The aim was to evaluate the importance of the transpiration of the bushes in the total savanna evapotranspiration rate. The grass layer characteristics are given in Table 1.

At this site, the shortwave reflected solar radiation R_f above the studied surfaces was measured using an inverted pyranometer (Kipp CM6). To evaluate the surface temperature, the emitted longwave radiation $\epsilon\sigma T_s^4$ was measured with a Model 4000 chopped thermoradiometer (Everest Interscience, Tucson, AZ, USA) at nadir position. A Q*6 net radiometer (Radiation Energy Balance System, Seattle, WA, USA) was mounted horizontally. All instruments were fixed on a horizontal 3 m arm fixed at 12 m on top of the flux station mast. The downward-looking radiometers respond to a cosine-weighted average of the incident fluxes upon the hemispherical windshield (Stannards et al., 1994). The measurements are spatial integrators representing an averaged value of the radiation budget of a sparse vegetation surface of some 1300 m² assuming the radiometers have an effective view angle of 120°. During the Intensive Observation Period (IOP), R_n and R_s were checked regularly to ensure the consistency of the measurements. The net radiometers used in the field were calibrated outdoors against a factory calibrated net radiometer.

Latent and sensible heat fluxes were calculated from the gradient of the mean values of the temperatures and water vapour pressures at the same levels through the energy budget–Bowen ratio method. Over the savanna area, the height of sampling was 4.5 m and 9.0 m; over the sparse grass layer, it was 0.2 m and 1.2 m above the canopy (Table 1). Temperatures were measured with shielded copper–constantan thermocouples and the water vapour pressure was measured using a Vaisala HMP35A humidity sensor (Vaisala Inc., Helsinki, Finland). Air was sampled alternately by two pumps (ASF, Puchheim, Germany) at the two levels and drawn through Tygon tubes to a three-way solenoid valve which was activated every 150 s by a signal from the data logger. It diverted the flow through a capacitance hygrometer sensor (Cellier and Oliosio, 1993), inside a measurement chamber of about 1 cm³. To allow stabilization, measurements were excluded during the first 30 s following the switching of the flow, and then the air temperature and humidity in the chamber were measured every 10 s and converted immediately into vapour pressure by the data logger (Campbell Scientific). The values at each level were then averaged over 20 min intervals. The two pumps, the solenoid valve and the hygrometer were placed in a wooden box fixed on the mast between the two levels.

The average soil heat flux density G_0 was calculated from measurements of four soil heat flux plates (Campbell Scientific) placed at 2 cm below the soil. One plate was under a bush savanna area and the other three were beneath a sparse grass area. The mean heat flux storage between the surface and 2 cm was added to the average G to estimate G_0 , the average heat flux value at the surface (Passerat de Silans et al., 1997).

2.3.2.2. CO₂ measurement

2.3.2.2.1. *Bowen and assimilation ratios coupled with the energy budget.* Another ratio, defined as the ratio of CO₂ assimilation to latent heat flux density, $\varphi = \mu A / \lambda E$, can be derived from gradients of CO₂ concentration, $d\text{CO}_2$, and water vapour pressure, at least during daytime hours:

$$\varphi = \frac{\mu \chi \rho}{\lambda} \cdot \frac{d\text{CO}_2}{de}$$

with χ the molecular weight ratio of CO₂ to air and ρ the air density.

When coupled with the energy budget Eq. (1), β and φ lead to the determination of the latent heat, sensible heat and CO₂ assimilation fluxes when $d\text{CO}_2$ is measured (Denmead and Bradley, 1985; Anderson and Verma, 1986; Baldocchi et al., 1988):

$$\lambda E = (R_n - G) / (1 + \beta + \varphi) \quad (4')$$

$$H = \beta(R_n - G) / (1 + \beta + \varphi) \quad (5')$$

$$\mu A = \varphi(R_n - G) / (1 + \beta + \varphi) \quad (6)$$

A special underground laboratory was built for the CO₂ measurements to avoid the daily temperature amplitude which affects the IRGA stability as well as the air density of the samples.

Air was sampled at the same two heights as the temperature by two pumps and drawn via buried copper tubes to the laboratory at a constant flow rate of 5 l min⁻¹. The buried lines were at the soil temperature (30–31°C); high enough to prevent internal condensation during the experiment (dew-point temperature: 24–26°C) and to avoid density differences between the two airstreams, which can cause errors as large as 40% in the measurements of CO₂ exchange (Leuning et al., 1982). In the laboratory, a fraction of the air was diverted from both lines through desiccant columns of drierite (anhydrous calcium sulphate with an indicating dye) and passed through needle valve rotameters to adjust the flow rate to 1.5 l min⁻¹. The air was passed through porous (40 μm) ceramic dust filters before entering the two sample cells of the IR Gas Analyser (IRGA) (ADC III, Hoddesdon, UK). The analyser signal was recorded at a sampling interval of 5 s and then averaged over a 20 min interval. The zero drift of the IRGA was determined twice a day by drawing a known concentration of CO₂ in air (320 ppm) through both sample cells, thus giving a zero reading to correct the previous values. The analyser drift was linear between calibration times. The output scale was evaluated by passing a calibrated CO₂ gas into the cells. The scale of the analyser was obtained between two standard gas concentrations of 320 ppm and 360 ppm. No correction was required for the dried samples of air from the two heights brought to a common pressure and temperature (Webb et al., 1980).

From another mast, air was sampled at 11.5 m to record continuously the atmospheric CO₂ concentration. The air was pumped and drawn through 15 m copper line, buried at 0.5 m depth in the soil, at a flow rate of 4 l min⁻¹. This brought the temperature of the air sample to that of the soil and avoided the measurement complication caused by the daily air density fluctuation. A fraction of this air was dried, cleaned of dust and routed through a Binos analyser (Binos, Hanau, Germany). No corrections needed to be applied (Webb et

al., 1980; Baldocchi et al., 1988). The zero drift of this IRGA was checked twice a day by drawing a dry calibrated CO_2 -air mixture (360 ppm) through the sample cell. This region was not affected by CO_2 from fossil fuel consumption nor by grassland burning during the IOP.

2.3.2.2.2. Eddy correlation. A three-dimensional Solent sonic anemometer (Gill Instruments, Southampton, UK) coupled with a Li-Cor LI-6262 differential closed path IR gas analyser (Li-Cor Inc., Lincoln, NE, USA) (see Verhoef et al. (1996) for more details) was used to evaluate the net CO_2 flux μA by the eddy correlation technique.

2.3.2.3. Soil moisture measurements. Soil water content was obtained from 12 neutron probe access tubes, installed over an area of $300\text{ m} \times 300\text{ m}$ around the mast. Average soil water content of the savanna area was determined by integrating the moisture content measured every 0.1 m from the surface to 1 m depth and every 0.2 m from 1 m to 1.6 m depth. The maximum value S_m was derived by integrating the highest moisture profile occurring during the IOP for the 0.6 m layer depth, where the maximum root biomass was found. The ratio S/S_m expressed the soil water content relative to the maximum water content.

3. Results and discussion

Rainfall patterns affect both the temporal and spatial characteristics of the savanna ecosystem.

3.1. Surface energy partition

Two clear days have been selected (Fig. 2). Diurnal net radiation follows that of incoming solar radiation. The trend of soil heat flux differs in the afternoon hours owing to a bush shadowing one of the soil heat flux plates. Maximum downward soil heat flux was between 180 and 200 W m^{-2} . In fact, grass and bushes cover only 60% of the ground surface, even when the vegetation was completely developed. Components of the energy balance presented for the period from 07:00 to 17:00 h correspond to the period of

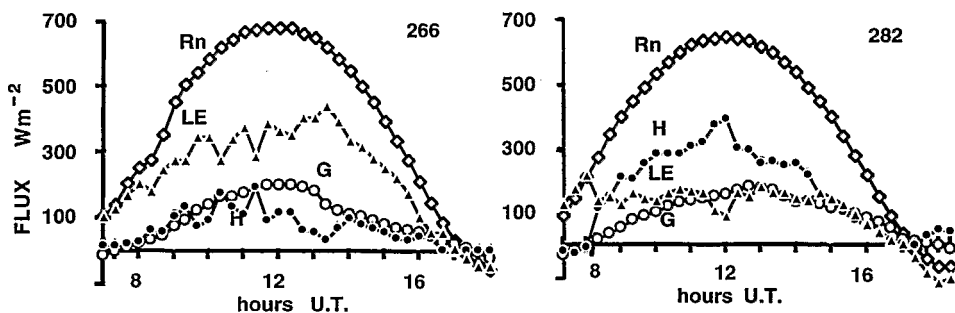


Fig. 2. Energy balance components of the savanna area during 2 days (the soil water content is a limiting factor on Day 282). R_n , Net radiation; LE, latent heat flux; H , sensible heat flux; G , soil heat flux.

positive net radiation. The partitioning of available energy ($R_n - G_0$) into latent and sensible heat fluxes of a well-watered young savanna vegetation (Day 266) show large values of λE with an average daily evaporative fraction ($EF_{8-16\text{ h}} = \sum \lambda E / \sum (R_n - G_0)$) of 0.85 for a soil water content of 78% of the maximum in the first 0.6 m depth and an LAI of 0.7. Atmospheric demand limits the vegetated layer energy exchange when soil water content is high.

When the soil water content has been depleted to 35–40% of the maximum in the first 0.6 m depth, and with some grass layer species into senescence (Day 282), the partitioning of the available energy $R_n - G_0$ is altered, with more sensible heat and less latent heat transferred to the atmosphere (Fig. 2). The daily evaporative fraction EF is 0.35. The trend observed between Days 261 and 282 is a general reduction of the latent heat flux from the surface to the atmosphere over 3 weeks, induced by the decrease in the soil water availability. The observed diurnal exchange processes over the Sahelian savanna surface depend on soil water content in the root zone as well as on the grass vegetation stage (age and LAI).

The average soil water content down to 1.6 m depth from Day 232 to Day 262 reflects rainwater infiltration (Fig. 3). At the end of the rainy season, a gradual drying out of the

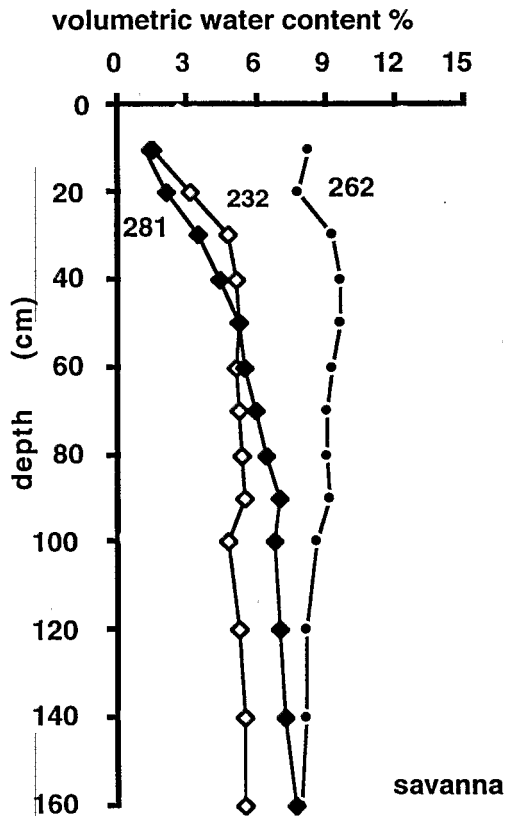


Fig. 3. Soil water content in the savanna area for three typical days during the Intensive Observation Period (IOP).

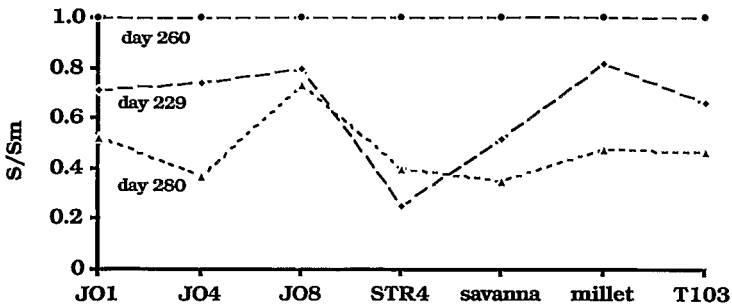


Fig. 4. Relative soil water content in a transect of 3.5 km in the catchment area for 3 days during the IOP. JO1, Edge of the laterite plateau; JO4, mid sandy skirt level between the plateau and the bottom of the valley; JO8, shelf of the valley, sandy loam, accumulating water from the gullies; STR4 and T103, valley floor with and without sandy crust at the surface.

soil was observed. The decrease in evapotranspiration during this period is due both to the reduction of the soil surface evaporation and to the decrease of the transpiration rate induced by the soil water depletion in the root zone (Table 1). Nearly 70% of the grass root system is located in the surface to 0.6 m soil layer. Fig. 4 shows the general decrease of the relative soil water content S/S_m in the catchment area. The transect of 3.5 km goes from the highest level of the catchment, JO1, passes through a spreading area, JO8, which is generally better watered than the savanna, and ends in the millet field area in the bottom of the valley.

Fig. 5 shows the evaporative fraction of the savanna area and its underlying grass layer for the complete IOP. At the start of the rainy period, the increase of the evaporative fraction is mainly due to surface soil water evaporation after rain, when grass cover is at the seedling stage. During a month (Days 239–269) when rainstorms contributed to a high soil water content over the area, the savanna evaporative fraction varied around 0.8 whereas the grass layer had a value of 0.65. The difference is attributed to the bush transpiration. The sparse grass layer represents the principal element in the energy

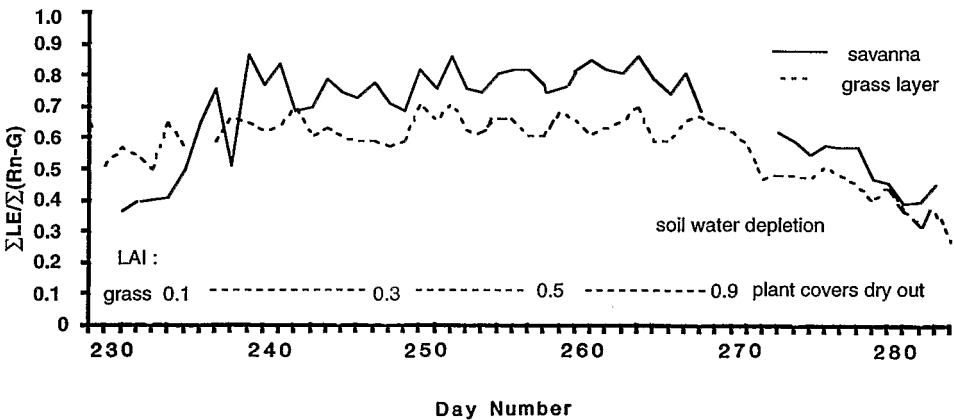


Fig. 5. The evaporative fraction of the savanna area and the underlying grass layer during the IOP.

exchange of the savanna surface. The evaporative fraction values are less than the usual value for well-watered conditions. Here, the main limiting factor on energy partition was the development of the leaf area for the vegetation as a whole. After Day 269, evaporation from the soil surface ceased some days after the last rain. When 30–40% of the available soil water was depleted, transpiration decreased progressively owing to the stomatal response of the grass layer to the water shortage. This was also observed during the Sahelian Energy Balance EXperiment (SEBEX) (Gash et al., 1991). With the drying cycle, the green leaf area of the vegetation decreases and the energy budget was modified, with more sensible heat being transferred to the atmosphere. The surface energy exchange was then controlled by the soil water content and not by the atmospheric demand.

The surface boundary-layer characteristics are affected as less evapotranspiration from the surface leads to less water vapour content in the atmospheric surface layer and more daytime sensible heat transfer from the surface increases the amplitude of variations in the air temperature over the region (Fig. 6). At the mesoscale, the water vapour pressure, e , decreases in the surface boundary layer as the air temperature increases, a process that begins at the same time as the soil water content starts to limit the vegetation transpiration rates all over the region. At the southern site, 54 km away, the same fluctuations of the atmospheric water vapour pressure and the air temperature were observed during this

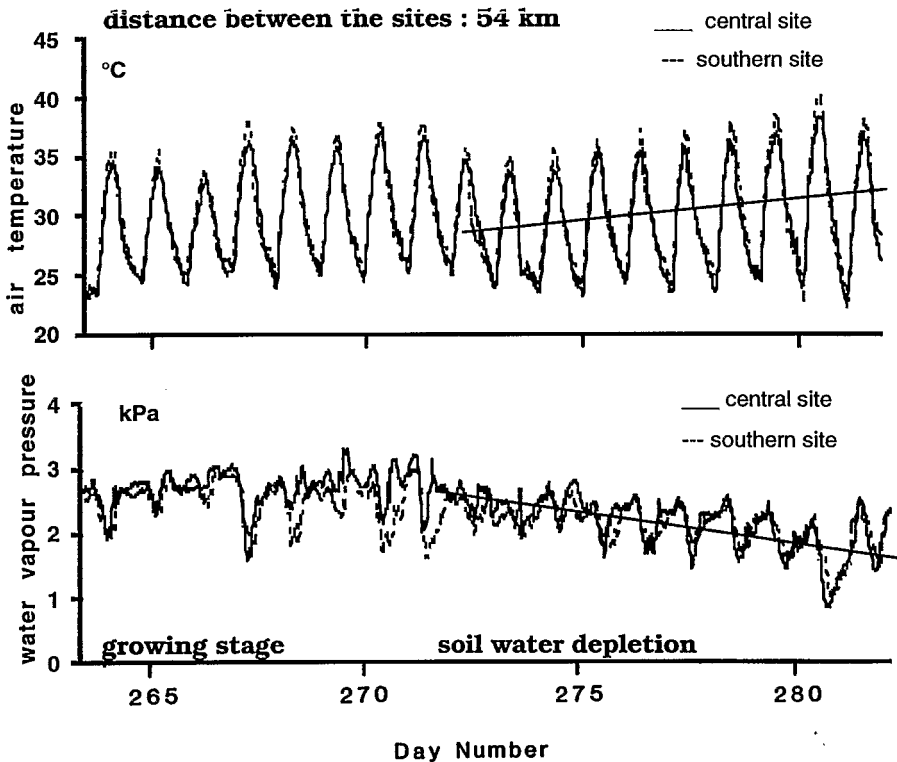


Fig. 6. Water vapour pressure, e , and the temperature in the surface boundary layer during the soil water depletion period in the Sahel for two locations 54 km apart.

period (Monteny et al., 1996). This shows the linkage between the biosphere evapotranspiration rates in relation to the soil water availability and the atmospheric characteristics of the surface boundary layer.

3.2. Parameterization development

The relationship between the Priestley-Taylor coefficient $\alpha = E/E_0$ and the relative soil water content S/S_m is nonlinear, as shown in Fig. 7. Soil moisture depletion affects the evapotranspiration rate E through an increase of the local large-scale surface resistance. The ratio E/E_0 decreases when nearly 30-40% of the total soil water is depleted in the root zone, so that soil water content controls the evaporative regime of the Sahelian land surface.

Parameterizations allow computation of the fluxes of radiation, sensible and latent heat at the land-surface-atmosphere interface in response to near-surface atmospheric conditions. The dependence of the savanna land surface behaviour on the soil water content (Fig. 7) can be determined by regression:

$$\alpha = \frac{E}{E_0} = 1.1 \left[1 - \exp\left(\frac{-1.7S/S_m}{1 - S/S_m}\right) \right] \tag{7}$$

The Priestley-Taylor coefficient α is related empirically to the soil water content. However, the equilibrium evaporation E_0 (Eq. (2)) has to be estimated to model the savanna evapotranspiration E . The radiation absorbed by the savanna area was evaluated using the incoming solar radiation. The net radiation R_n was derived from the following relation:

$$R_n = 0.71R_s - 1.7 \text{ (MJ m}^{-2} \text{ day}^{-1}) \quad r^2 = 0.99 \tag{8}$$

where R_s is the total downward solar radiation flux density (hourly data integrated over a day) measured during this experiment (mid-August until end of September).

Because of the poor soil coverage by plant grasses, plants and bush foliage, the soil heat flux of the Sahelian surface (G_0) represents nearly 30% of the net radiation when averaged

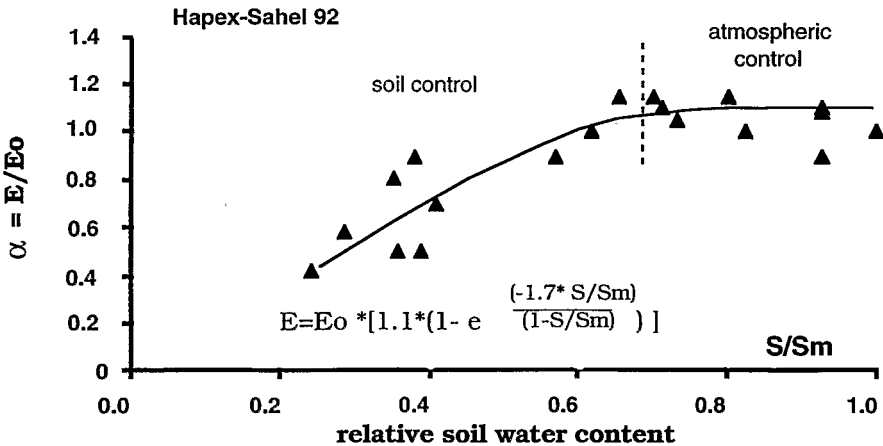


Fig. 7. Relationship between the ratio E/E_0 (daily values) and the relative soil water content S/S_m .

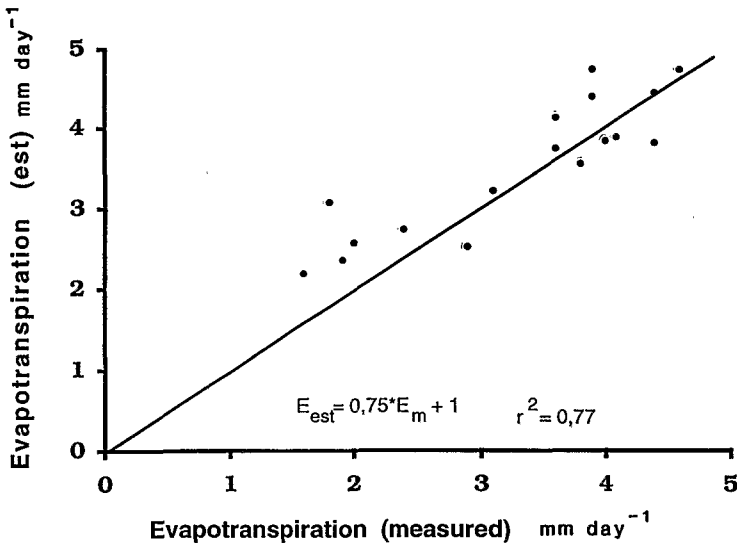


Fig. 8. Relationship between the measured evapotranspiration rate of the savanna area and the estimated evapotranspiration obtained by Eq. (12).

over a diurnal cycle (07:00–19:00 h):

$$G_0 = 0.3R_n - 1.1 \text{ (MJ m}^{-2} \text{ day}^{-1}) \quad r^2 = 0.88$$

Therefore, the available energy is represented by

$$R_n - G_0 = 0.49R_s - 0.1 \text{ (MJ m}^{-2} \text{ day}^{-1}) \tag{9}$$

The equilibrium evaporation, E_0 , is expressed (Eq. (2)) as

$$E_0 = \left(\frac{s}{s + \gamma} \right) \left[0.49 \left(\frac{R_s - 0.1}{\lambda} \right) \right] \tag{10}$$

and the evapotranspiration E can be formulated by combining the former equations as follows:

$$E_{est} = \left[\frac{0.49(R_s - 0.1)}{\lambda} \right] \left(\frac{s}{s + \gamma} \right) \cdot \left[1 - \exp\left(\frac{-1.7S/S_m}{1 - S/S_m} \right) \right] \text{ (mm day}^{-1}) \tag{11}$$

The daily evapotranspiration rate E_{est} thus obtained is compared with the measured values E_m in Fig. 8. The scattering around the 1:1 line shows that the model performs correctly although it overestimates small daily values of evaporation. These expressions allow computation of the savanna evapotranspiration rate, E , from the rainfall, which contributes to the soil water content, and from the incoming solar radiation (both climatic forcing factors) for the Sahelian land surface.

By considering that the region behaves as an uniform hydrological unit in respect of soil water content, Eq. (11) provides information about the water exchange rate for the grid scale. An estimation of spatial and temporal variation of the evaporation may be obtained

by combining Eq. (11) with the midday radiometric surface temperature obtained from remote sensing (Monteny et al., 1994; Amram et al., 1995). The soil water depletion modifies the biosphere evapotranspiration and CO_2 exchange rates by increasing the surface resistance and later on by reducing the active green leaf area.

3.3. CO_2 downward flux

The downward CO_2 fluxes for two selected days are shown in Fig. 9: a clear day with soil moisture fully recharged (Day 266) and a clear day with moisture shortage (Day 282). The pattern of photosynthesis of the canopy during the daylight hours (Day 266) is not symmetrical in shape; it increases quickly in the morning until 10:00–11:00 h, to a value around $10 \mu\text{mol CO}_2 \text{ m}^{-2} \text{ s}^{-1}$, then decreases slowly after 15:00 h. This is for a savanna where the grass layer had an LAI of 0.70 (Table 1). The rapid increase could be due to the turbulence, which affects the CO_2 air concentration in the morning near the surface, reducing it from 350 ppm at 08:00 h to 335 ppm at 10:00 h. The CO_2 exchange rate values for non-limiting soil water content are lower than those quoted in the literature for crops or grass prairie area (Verma et al., 1989; Verma et al., 1992). It is not only the LAI of the grass layer which limits the assimilation rate but also its structure, because erect leaves intercept very little photosynthetically active radiation (Bégué et al., 1994, Bégué et al., 1997).

With soil water depletion, a general decrease in CO_2 assimilation is seen as the grass layer proceeds towards water stress conditions (Day 282). The stomatal resistance rises, reducing the atmospheric CO_2 and latent heat transfer. This, in turn, increases the vegetated surface temperature, which acts on the respiration process by reducing the net CO_2 assimilation rate of the grass layer. The low value of the canopy CO_2 assimilation on Day 282 results from the combination of the depletion of the soil water content and the respiration rates. The observed general decrease in CO_2 assimilation rate and water vapour

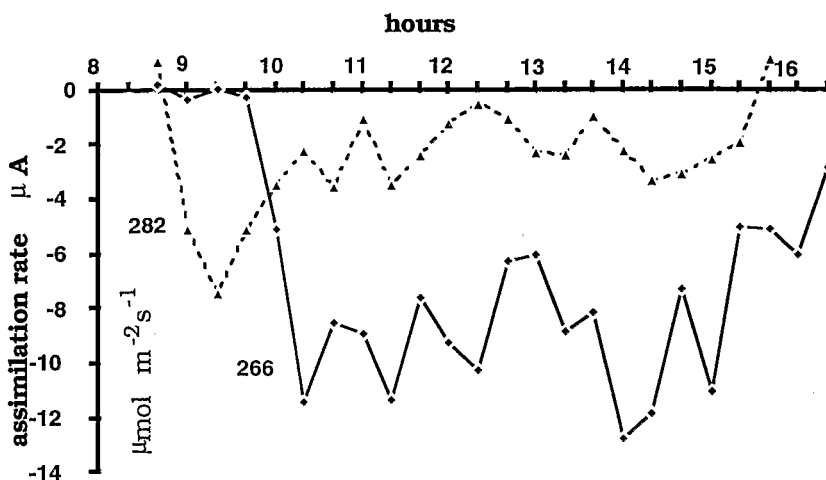


Fig. 9. Diurnal pattern of the savanna CO_2 assimilation rate for two contrasting soil water conditions.

transfer comes particularly from the savanna grass layer, which is affected by soil water depletion 2–3 weeks after the rainfall events (Fig. 3). Similar observations have been made at the other sites (Verhoef et al., 1996; Moncrieff et al., 1997). The CO₂ flux from the soil was not measured, so the results do not express the composite net assimilation rate of the savanna surface.

The regression equation relating the net assimilation rate of the savanna land area and the incoming PAR is shown as a continuous line and compared with experimental points from central sites and in relation to the soil water availability S/S_m (Fig. 10). The relationship has the rectangular hyperbola form:

$$\mu A = \left[\frac{a \left(\frac{S}{S_m} \right) \text{PAR}}{a \left(\frac{S}{S_m} \right) + \text{PAR}} \right] + c \tag{12}$$

with $a = -22$, $b = -0.045$, $c = 6.5$ and S/S_m the relative soil water content.

For high soil water content ($S/S_m > 0.85$), the adjusted curve is a rectangular hyperbolic curve with an asymptotic character, with light saturation at 1600–1800 $\mu\text{mol m}^{-2} \text{s}^{-1}$ for a radiative surface temperature between 36 and 42°C. When neither soil water nor temperature is limiting photosynthesis, the assimilation rate vs. the incoming PAR indicates the potential of the savanna to absorb the atmospheric CO₂ (Eq. (12)). In the intercomparison paper (Moncrieff et al., 1997), a comparable hyperbolic fit of CO₂ flux data vs. PAR is presented for millet. At intermediate values of the soil water content ($S/S_m \approx 0.75$), the

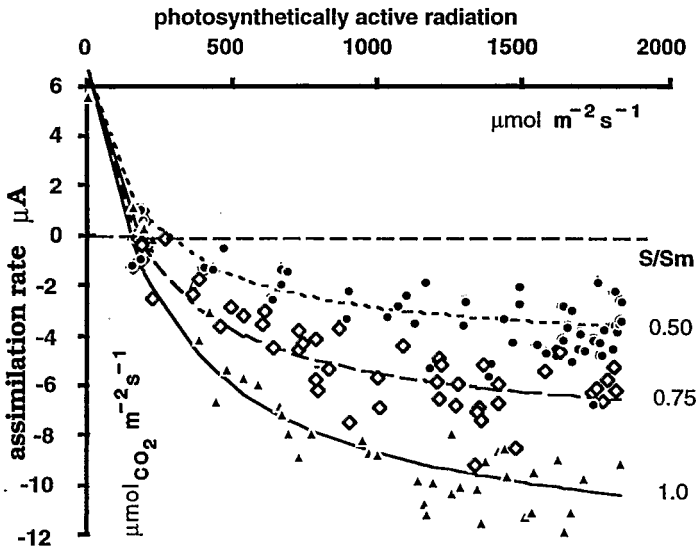


Fig. 10. Relationship between net assimilation rate of the savanna land area and the photosynthetically active radiation input with respect to the soil water availability S/S_m . The fitted curve is a theoretical line when neither water stress nor temperature limit photosynthesis. The dashed horizontal line represents the equilibrium between assimilation and respiration rates.

experimental points show a decrease in the assimilation rate. The reduction of the availability of soil water induces an increase of the general surface resistance. This raises the surface temperature to values between 40 and 46°C during the day. As soil moisture decreases further during the early senescent stage, the shift to smaller net assimilation rates in the experimental points is the result of the interactions between soil moisture content ($S/S_m < 0.5$) which controls the stomatal aperture, increasing the surface resistance which raises the surface temperature to values between 44 and 51°C. This reduces the green leaf area to $LAI \approx 0.45$. In Fig. 10, the result of the parameterization described in Eq. (12) is given by the dotted fitting curves. The rates of CO_2 assimilation by the vegetation are well described by the above parameterization, which is related to incoming PAR as well as to soil water content in the root zone.

The general trend is a large reduction of the surface CO_2 flux density with depletion of the soil water content, although plant species can still photosynthesize at high temperatures, as shown by the results. The daily net downward CO_2 flux $\Sigma\mu A$ (08:00–16:00 h) decreases from 8 to 2 g CO_2 m⁻² at the end of the IOP when the green leaf area diminishes. The soil moisture content in the root zone is the state variable that controls the magnitude of the surface fluxes through the canopy surface resistance. The relation between soil water availability and CO_2 assimilation is complex, considering the secondary effects on the photosynthesis processes. The parameterization of the surface energy balance components (sensible and latent heat fluxes and net photosynthesis rate) of a semi-arid savanna land surface also provides links to surface radiometric temperature and the available soil water content (Monteny et al., 1994; Amram et al., 1995).

The development of the photosynthetic activity of the savanna land area during the growth is characteristic of the global water and CO_2 exchanges over the Sahelian region. During the wet season, the land surface is a sink for atmospheric carbon, which is tied up in

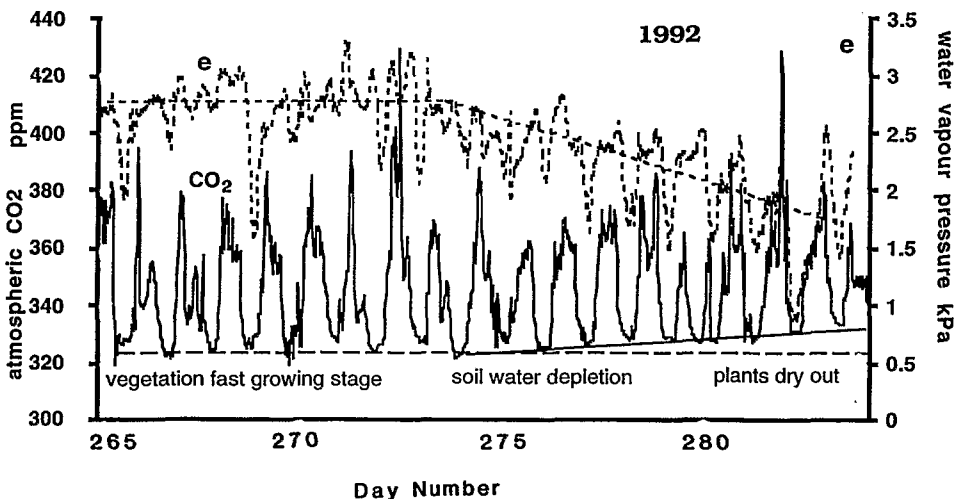


Fig. 11. Soil water depletion affects the energy exchange rates of the savanna land area, which reduces the atmospheric water vapour and increases the CO_2 concentrations during the IOP. Data were measured at 12 m above the savanna area.

the biomass reservoir during the growing period when soil water is available in the root zone (Table 1).

3.4. Impact on the atmospheric parameters

Fig. 11 presents the general evolution of the atmospheric CO₂ concentration from the end of the rainy season until the vegetation has dried out. The atmospheric water vapour pressure, e , varied from day to day but the average value is nearly constant during the fast growing stage of the vegetation. With soil water depletion in the 0–0.6 m soil layer, the evapotranspiration rate from all vegetated surfaces of the region decreases and affects the atmospheric water vapour concentration. The reduction of CO₂ assimilation by the savanna cover during daylight hours induces an increase of the atmospheric CO₂ concentration. The daily amplitude of the CO₂ signal is clearly indicated. Nocturnal plant respiration and soil CO₂ emission increase the atmospheric CO₂ concentration to a maximum in the early morning. Before sunrise, with low turbulence, the morning level of atmospheric CO₂ concentration may reach 360–390 ppm. After sunrise, plant cover assimilation and vertical mixing effects are very pronounced and the atmospheric CO₂ concentration is reduced to a value of 320–330 ppm. It is generally less than the monthly mean atmospheric CO₂ concentration value of 340 ppm at this latitude (Fung et al., 1983). During daytime hours, vigorous mixing dynamics make the CO₂ concentration in the atmosphere highly conservative. With the general decrease in the soil water content all over the region, the CO₂ absorbed by the surface is reduced and the atmospheric CO₂ concentration increases progressively. The influence of the ground area as source (water vapour) and sink (CO₂) weakens. The atmospheric CO₂ content can be considered as an integrator of the physiological activity at the regional scale (Goudriaan, 1987). The seasonal CO₂ cycle, like the diurnal cycle, is of biospheric origin. During both the wet and dry seasons, the Sahelian biosphere is an active driving force in the regional water and carbon cycles.

4. Conclusion

Micrometeorological data were measured during the rainy season and at the beginning of the dry period. The flux stations provided temporal information about the development of the exchange processes of the savanna.

In a semi-arid region, the major driving variable is the amount and temporal distribution of the rainfall, and the main state variables are the composition and evolution of the vegetation and the soil water availability. Both these variables control the partitioning of the available energy into sensible and latent heat fluxes and CO₂ assimilation rate. For a well-watered savanna vegetation, water vapour transfer from the savanna to the atmosphere represents 75–80% of the available energy, of which 65% originates from the grass layer. The assimilation rate represents only 0.6% of the PAR because of the structure of the grass layer (erect leaves and low LAI). The net CO₂ downward daily evolution of the savanna area decreases progressively with the depletion of the soil water availability in the root zone of the grass species.

With decreasing soil water content in the 0–0.6 m soil layer, the energy budget partitioning is modified and more sensible heat is transferred to the atmosphere, inducing a greater air temperature amplitude. The water stress increases the stomatal resistances so that surface temperatures rise, and, at midday, mean surface temperatures were usually greater than 42°C, higher than the optimum for photosynthesis. Plant respiration increases and the assimilation rate decreases. The deficit in soil water leads to a progressive reduction of the CO₂ assimilation by the vegetation.

The seasonal pattern of the downward CO₂ flux of the savanna canopy shows an increase in the assimilation with the growth of the plant species in the grass layer. As soil water availability in the grass root zone decreases, so the CO₂ assimilation decreases and the increase of the radiative surface temperature accentuates the reduction in the canopy assimilation rate. Thus, at the end of the rainy season, when senescence or water stress of the vegetation occurs, the mean atmospheric CO₂ concentration increases. Sizeable diurnal fluctuations of atmospheric CO₂ concentration can be observed in the lowest few metres of the surface boundary layer.

The atmospheric CO₂ can be considered as an integrated parameter in this continental region if the full atmospheric column is taken into account. By assuming that large savanna land areas respond as uniform hydrological units, the proposed submodels (Eq. (8), Eq. (9), Eq. (11) and Eq. (12)) can be used to evaluate the evaporation rates, and the CO₂ assimilation rates can provide information required by atmospheric models at the regional scale.

References

- Adamou, M.R., 1992. Dynamique saisonnière de la strate herbacée le long d'un gradient successional dans les savannes jachères du Sahel nigérien. Rapport de stage, Université de Niamey.
- Amram, O., Cherchali, S., Flouzat, G. and Monteny, B.A., 1995. Integration of the spatio-temporal heterogeneity of ecosystems to improve the hydrological fluxes. IGARSS'95, 10–14 July, Florence.
- Anderson, D. and Verma, S., 1986. Carbon dioxide, water vapor and sensible heat exchanges of a grain sorghum canopy. *Boundary-Layer Meteorol.*, 34: 317–331.
- Baldocchi, D., Hicks, B. and Meyers, T., 1988. Measuring biosphere–atmosphere exchanges of biologically related gases with micrometeorological methods. *Ecology*, 69: 1331–1340.
- Bégué, A., Hanan, N.P. and Prince, S.D., 1994. Radiative transfer in shrub savanna sites in Niger. Preliminary results from HAPEX-Sahel. 2. Photosynthetically active radiation interception of the woody layer. *Agric. For. Meteorol.*, 69: 247–266.
- Bégué, A., Hanan, N.P. and Prince, S.D., 1997. Intercepted photosynthetically active radiation and spectral vegetation indices in HAPEX-Sahel. *J. Hydrol.*, this issue.
- Cellier, P. and Olioso, A., 1993. A simple system for automated longterm Bowen ratio measurement. *Agric. For. Meteorol.*, 66: 81–92.
- De Bruin, H.A.R., 1983. A model for the Priestley–Taylor parameter *a*. *J. Clim. Appl. Meteorol.*, 22: 572–578.
- Denmead, O.T. and Bradley, E.F., 1985. Flux gradient relationships in a forest canopy. In: B. Hutchison and B. Hicks (Editors), *The Forest–Atmosphere Interaction*. D. Reidel, Dordrecht, pp. 421–442.
- Denmead, O.T. and McIlroy, I.C., 1971. Measurement of carbon dioxide exchange in the field. In: Z. Sestak, J. Catsky and P.G. Jarvis (Editors), *Plant photosynthetic production*, pp. 367–514.
- Fung, I.Y., Prentice, K., Matthews, E., Lerner, J. and Russel, G., 1983. Three-dimensional tracer model study of atmospheric CO₂: response to seasonal changes with the terrestrial biosphere. *J. Geophys. Res.*, 88: 1281–1294.

- Gash, J.H.C., Wallace, J.S., Lloyd, C.R., Dolman, A.J., Sivakumar, M.V. and Renard, C., 1991. Measurements of evaporation from fallow Sahelian savannah at the start of the dry season. *Q. J. R. Meteorol. Soc.*, 117: 749–760.
- Goudriaan, J., 1987. The biosphere as a driving force in the global carbon cycle. *Neth. J. Agric. Sci.*, 35: 177–187.
- Goutorbe, J.P., Lebel, T., Tinga, A., Bessemoulin, P., Brouwer, J., Dolman, A.J., Engman, E.T., Gash, J.H.C., Hoepffner, M., Kabat, P., Kerr, Y.H., Monteny, B.A., Prince, S., Said, F., Sellers, P. and Wallace, J.S., 1994. HAPEX-Sahel: a large scale study of land–atmosphere interactions in the semi-arid tropics. *Ann. Geophys.*, 12: 53–64.
- Goutorbe, J.P., Lebel, T., Dolman, A.J., Gash, J.H.C., Kabat, P., Kerr, Y.H., Monteny, B., Prince, S.D., Stricker, J.N.M., Tinga, A., and Wallace, J.S., 1997. An overview of HAPEX-Sahel: a study in climate and desertification. *J. Hydrol.*, this issue.
- Jarvis, P.G., James, G.B. and Lansberg, J.J., 1976. Coniferous forest. In: J.L. Monteith (Editor), *Vegetation and the Atmosphere*, Vol. 2. Academic Press, London, pp. 171–236.
- Leroux, M., 1983. *The Climate of Tropical Africa*. Champion, Paris.
- Leuning, R., Denmead, O., Lang, A.R. and Ohtaki, E., 1982. Effects of heat and water vapour transport on eddy covariance measurements of CO₂ fluxes. *Boundary-Layer Meteorol.*, 23: 209–222.
- Lhomme, J.P., Monteny, B.A. and Amadou, M., 1994a. Estimating sensible heat flux from radiometric temperature over sparse millet. *Agric. For. Meteorol.*, 68: 77–91.
- Lhomme, J.P., Monteny, B.A., Chehbouni, A. and Troufleau, D., 1994b. Determination of the heat flux over sahelian fallow savanna using infrared thermometry. *Agric. For. Meteorol.*, 68: 93–105.
- Moncrieff, J.B., Monteny, B., Verhoef, A., Friborg, Th., Elbers, J., Kabat, P., de Bruin, H., Soegaard, H., Jarvis, P.G. and Taupin, J.D., 1997. Spatial and temporal variations in net carbon flux during HAPEX-Sahel. *J. Hydrol.*, this issue.
- Monteny, B.A., 1993. HAPEX-Sahel: campagne de mesures sur le SuperSite Central Est. Synthèse des participations et résultats préliminaires. Rapport ORSTOM, Montpellier, 220 pp.
- Monteny, B.A. and Casenave, A., 1989. The forest contribution to the hydrological budget in tropical West Africa. *Ann. Geophys.*, 7: 427–436.
- Monteny, B.A., Lhomme, J.P., Sicot, M., Amadou, M., Chehbouni, A. and LeRoux, X., 1994. Parametrization of the energy exchange processes over a semi-arid sahelian vegetated surface. *European Conference on the Global Energy and Water Cycle (GEWEX)*, 18–22 July 1994. Royal Meteorological Society, London.
- Monteny, B.A., Lhomme, J.P., Chehbouni, A., Amadou, M., Troufleau, D., Brunel, J.P., Bessemoulin, P., Sicot, M., Galle, S., Lloyd, C.R. and Said, F., 1996. Les interactions surface continentale–atmosphère en milieu sahélien. Passage de l'échelle stationnelle à l'échelle régionale. Colloques et Séminaires, ORSTOM, Montpellier.
- Nichols, W.E. and Cuenca, R., 1993. Evaluation of the evaporative fraction for parametrization of the surface energy balance. *Water Resour. Res.*, 29: 3681–3690.
- Passerat de Silans, A., Monteny, B.A. and Lhomme, J.P., 1997. The correction of soil heat flux measurements to derive an accurate surface energy balance by the Bowen ratio method. *J. Hydrol.*, this issue.
- Priestley, C.H. and Taylor, R.J., 1972. On the assessment of surface heat flux and evaporation using large scale parameters. *Mon. Weather Rev.*, 100: 81–92.
- Prince, S., Kerr, Y.H., Goutorbe, J.P., Lebel, T., Tinga, A., Bessemoulin, P., Brouwer, J., Dolman, A.J., Engman, E.T., Gash, J.H.C., Hoepffner, M., Kabat, P., Monteny, B.A., Said, F., Sellers, P. and Wallace, J.S., 1995. Geographical, biological and remote sensing aspects of the Hydrological Atmospheric Pilot Experiment in the Sahel (HAPEX-Sahel). *Remote Sens. Environ.*, 51: 215–234.
- Stannards, D.I., 1993. Comparison of Penman–Monteith, Shuttleworth–Wallace and modified Priestley–Taylor evapotranspiration models for wildland vegetation in semi-arid rangeland. *Water Resour. Res.*, 29: 1379–1392.
- Stannards, D.I., Blanford, J.H., Kustas, W.P., Nichols, W.D., Amer, S.A., Schmutge, T.J. and Weltz, M.A., 1994. Interpretation of surface flux measurements in heterogeneous terrain during the Monsoon '90 experiment. *Water Resour. Res.*, 30: 1227–1239.
- Verhoef, A., Allen, S., de Bruin, H.A.R., Jacobs, M.J. and Heusinkveld, B.G., 1996. Fluxes of carbon dioxide and water vapour from a sahelian savanna. *Agric. For. Meteorol.*, 80: 231–248.

- Verma, S., Kim, J. and Clement, R., 1989. Carbon dioxide, water vapor and sensible heat fluxes over a tall grass prairie. *Boundary-Layer Meteorol.*, 46: 53–67.
- Verma, S., Kim, J. and Clement, R., 1992. Momentum, water vapor and carbon dioxide exchange at the centrally located prairie site during FIFE. *J. Geophys. Res.*, 97: 18629–19639.
- Wallace, J.S., Wright, I.R., Stewart, J.B. and Holwill, C.J., 1991. The Sahelian energy balance experiment SEBEX: ground based measurements and their potential for spatial extrapolation using satellite data. *Adv. Space Res.*, 11: 131–141.
- Webb, E.K., Pearman, G.I. and Leuning, R., 1980. Correction of flux measurements for density effects due to heat and water vapour transfer. *Q. J. R. Meteorol. Soc.*, 106: 85–100.



Notes to contributors

A detailed *Guide for Authors* is available upon request from the Publisher, Elsevier Editorial Services, Mayfield House, 256 Banbury Road, Oxford OX2 7DH, UK, and will also be printed each year (for 1997: Vol. 187, Nos. 1–2). Please pay attention to the following notes:

Language

The official language of the journal is English.

Preparation of the text

- (a) The manuscript should preferably be prepared on a word processor and printed with double spacing and wide margins and include an abstract of not more than 500 words.
- (b) The title page should include the name(s) of the author(s), their affiliations, fax and e-mail numbers. In case of more than one author, please indicate to whom the correspondence should be addressed.

References

- (a) References in the text consist of the surname of the author(s), followed by the year of publication in parentheses. All references cited in the text should be given in the reference list and vice versa.
- (b) The reference list should be in alphabetical order and on sheets separate from the text.

Tables

Tables should be compiled on separate sheets and should be numbered according to their sequence in the text.

Illustrations

- (a) All illustrations should be numbered consecutively and referred to in the text.
- (b) Drawings should be lettered throughout, the size of the lettering being appropriate to that of the drawings, but taking into account the possible need for reduction in size. The page format of the journal should be considered in designing the drawings.
- (c) Photographs must be of good quality, printed on glossy paper.
- (d) Figure captions should be supplied on a separate sheet.
- (e) If contributors wish to have their original figures returned this should be requested at proof stage at the latest.
- (f) Colour figures can be accepted providing the reproduction costs are met by the author. Please consult the publisher for further information.

Proofs

One set of proofs will be sent to the corresponding author, to be checked for typesetting/editing. The author is not expected to make changes or corrections that constitute departures from the article in its accepted form.

Page charges and reprints

There will be *no page charge*. Each author receives with his galley proofs a reprint order form which must be completed and returned to the Publisher *with* the proofs, Elsevier Editorial Services, Mayfield House, 256 Banbury Road, Oxford OX2 7DH, UK, tel. (1865) 314900; telefax (1865) 314990. Additional reprints (minimum 100) can be ordered at quoted prices. *Fifty reprints* of each article are supplied *free of charge*.

Submission of manuscripts

One original and two copies should be submitted to: Editorial Office, Journal of Hydrology, P.O. Box 1930, 1000 BX Amsterdam, The Netherlands. The indication of a fax and e-mail number on submission of the manuscript could assist in speeding communications. Illustrations: Please note that on submission of a manuscript **three sets** of all photographic material printed **sharply on glossy paper** or as **high-definition laser prints** must be provided to enable meaningful review. Photocopies and other low-quality prints will not be accepted for a review. Submission of an article is understood to imply that the article is original and unpublished and is not being considered for publication elsewhere. Upon acceptance of an article by the journal, the author(s) will be asked to transfer the copyright of the article to the publisher. This transfer will ensure the widest possible dissemination of information.

Authors in Japan please note: Upon request, Elsevier Science Japan will provide authors with a list of people who can check and improve the English of their paper (*before* submission). Please contact our Tokyo office: Elsevier Science Japan, 9–15 Higashi-Azabu, Minato-ku, Tokyo 106. Tel: (03)-5561-5033, Fax (03)-5561-5047.

Submission of electronic text

In order to publish the paper as quickly as possible after acceptance, authors are encouraged to submit the final text also on a 3.5" or 5.25" diskette. Both double density (DD) and high density (HD) diskettes are acceptable. Make sure, however, that the diskettes are formatted according to their capacity (HD or DD) before copying the files onto them. Similar to the requirements for manuscript submission, main text, list of references, tables and figure legends should be stored in separate text files with clearly identifiable file names. The format of these files depends on the word processor used. Texts made with DisplayWrite, MultiMate, Microsoft Word, Samna Word, Sprint, Volkswriter, Wang PC, WordMARC, WordPerfect, Wordstar, or supplied in DCA/RFT, or DEC/DX format can be readily processed. In all other cases the preferred format is DOS text or ASCII. It is essential that the name and version of the wordprocessing program, type of computer on which the text was prepared, and format of the text files are clearly indicated. Authors are requested to ensure that the contents of the diskette correspond exactly to the contents of the hard copy manuscript. Discrepancies can lead to proofs of the wrong version being made. The word processed text should be in single column format. Keep the layout of the text as simple as possible; in particular, do not use the word processor's options to justify or to hyphenate the words. If available, electronic files of the figures should be included on a separate floppy disk.

General Information

Back volumes, orders and information requests should be addressed to Elsevier Science B.V., Journals Department, P.O. Box 211, 1000 AE Amsterdam, Netherlands. *Back volumes are available on microfilm*. Orders and information requests concerning back volumes on microfilm should be addressed exclusively to: Elsevier Science Inc., Journal Information Center, 655 Avenue of the Americas, New York, NY 10010, USA.

Customers in the USA and Canada requiring additional bibliographic information on this and other Elsevier journals, please contact Elsevier Science Inc., Journal Information Center, 655 Avenue of the Americas, New York, NY 10010, USA, tel. (212) 633-3750; fax. (212) 633 3764; telex. 420-643 AEP UI.

US mailing notice – *Journal of Hydrology* (ISSN 0022 1694) is published monthly by Elsevier Science B.V., (Molenwerf 1, Postbus 211, 1000 AE Amsterdam). Annual subscription price in the USA US\$3475.00 (valid in North, Central and South America), including air speed delivery. Application to mail at second class postage rate is paid at Jamaica, NY 11431.

USA POSTMASTERS: Send address changes to *Journal of Hydrology* Publications Expediting, Inc., 200 Meacham Avenue, Elmont, NY 11003. **AIRFREIGHT AND MAILING** in the USA by Publications Expediting, Inc., 200 Meacham Avenue, Elmont, NY 11003.

